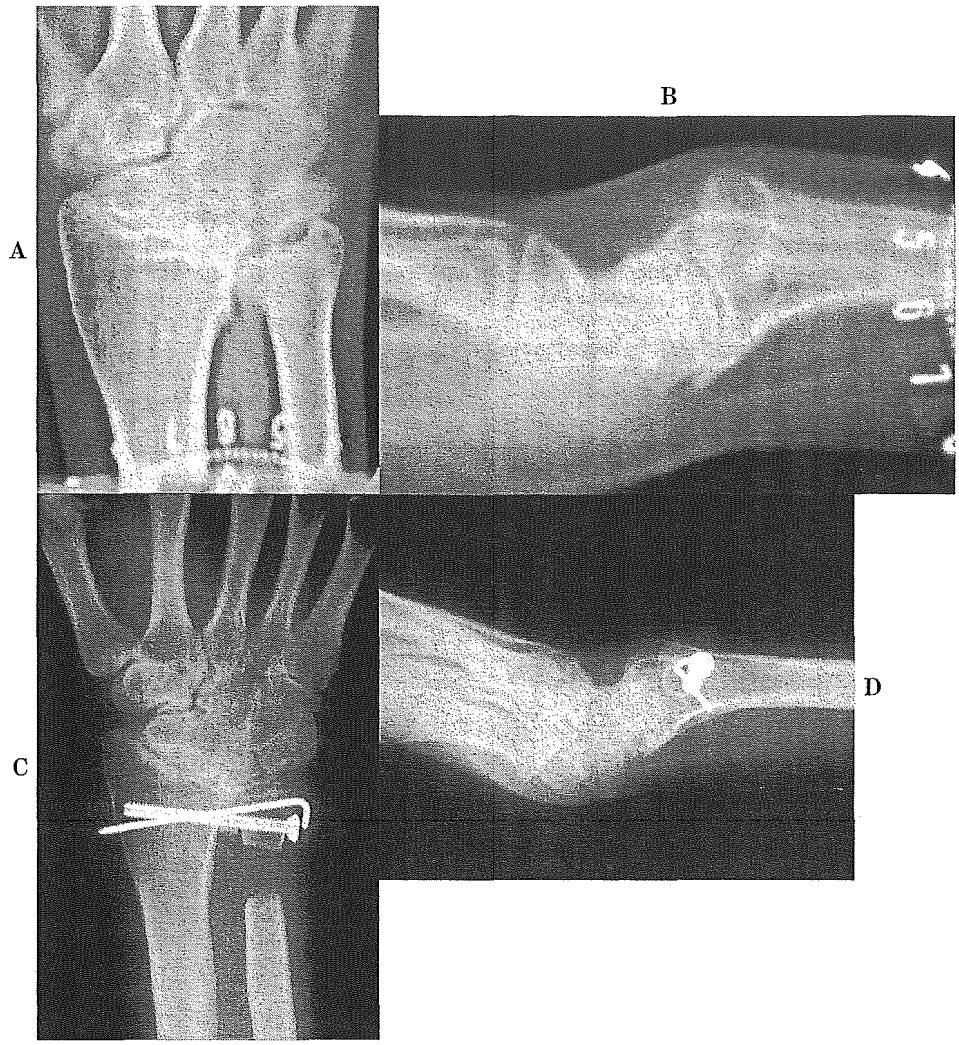

図 8　60 歳女性，右 RA 手関節，stage Ⅳ．(A)術前正面断層写真．(B)術前側面断層写真．(C)Sauvé-Kapandji 手術後 2 年の正面 X 線写真．遠位橈尺関節部の骨癒合は得られている．(D)Sauvé-Kapandji 手術後 2 年の側面 X 線写真．尺骨遠位端の亜脱臼も整復されている．

スクリュー 1 本を加えて固定する．尺骨骨切り部の骨膜は完全に切除し，尺骨骨切り部の再癒合を防止する(図 8-A, B, C, D)．骨癒合が得られるまで外固定を継続すべきとの報告もあるが，著者は全例，2 週間の外固定のみで遠位橈尺関節が偽関節に陥った例はなかった．

S-K 手術の問題点として，Darrach 手術と同様に尺骨近位端の不安定性によるクリック，疼痛などがあげられる．不安定性が著明な場合，尺骨近位端と橈骨が衝突(impinge)する．著者は Darrach 手術の項で記載した ECU 腱の半切腱を用いた切除端安定化術を S-K 法による尺骨近位端安定化にも応用して行っており[15]，尺骨近位端の不安定性の制御が得られている(図 9)．

③Hemiresection interposition arthroplasty (Bowers 手術)[13),18)]

比較的早期の RA 手関節で TFCC の機能が温存されているが，遠位橈尺関節での滑膜炎による回旋時痛が著明な場合が適応となる．したがって，RA 手関節では遠位橈尺関節，TFCC が侵されていることが多いので適応となることは少ないと思われる．

手術方法は尺骨の TFCC 付着部を温存して尺骨頭の橈骨との関節面を切除し，切離した関節包および伸筋支帯を尺骨頭の切除面に介在するように縫合する．長掌筋腱の腱球を挿入する場合もある．伸筋支帯を尺側と橈側に茎部を有する交互の弁として挙上して，小指伸筋腱および ECU 腱を反転して遠位橈尺関節背側関節

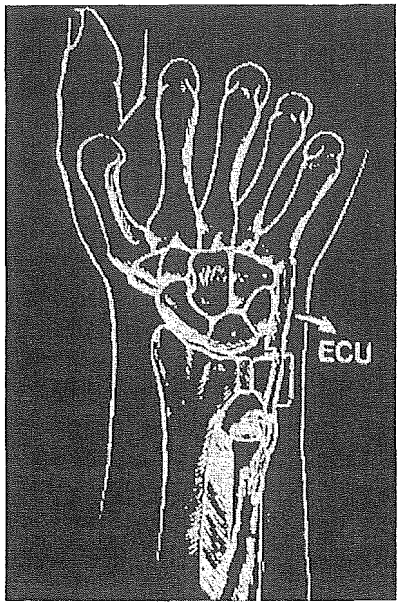

図9 Sauvé-Kapandji手術後の尺骨遠位端に対するECU腱半切腱を用いた安定化術.

包を露出する．関節包を橈骨の尺骨切痕部で切離して尺骨頭の橈側半分を切除する．切除した空隙に背側関節包あるいは長掌筋腱を介在物として挿入する(図10-A, B, C)．Bowersは反転したECU腱を伸筋支帯を用いて中心化術を行ったが，著者の経験ではこれにより術後に高頻度にECU腱炎が発生したために，最近ではECU腱を展開せずに行うことによりこの問題は解決している．術後の外固定などはS-K手術と同様である．

3) 橈骨手根関節の再建術

①橈骨月状骨(radio-lunate: RL)固定術

橈骨手根関節の破壊による手関節掌背屈での疼痛が強く，手根中央関節は比較的保たれている例が適応となる．また，術前手根骨の尺側偏位や橈側回旋が見られる場合にDarrach手術を行う際は，手関節の適合性の矯正と変形の進行を防止する目的でRL固定術を追加することが多い．橈骨舟状骨関節も強く侵されている場合は橈骨舟状月状骨(radio-scaphoid-lunate: RSL)固定術も適応となるがRSL固定術は動きが強く抑制されるので，著者はRL固定術を好んで用いている．手根中央関節が温存されており，橈骨舟状骨関節が比較的温存されているが，橈骨月状骨関節での破壊が著明な場合がRL固定術のもっともよい適応と考えている．

橈骨月状骨窩および月状骨近位関節面の軟骨および骨皮質を海綿骨が露出するまで切除したのち，月状骨を解剖学的に整復する．手根骨全体の尺側偏位，橈側回旋を矯正するように留意する．腸骨あるいはDarrach手術によって得た尺骨頭をブロック状に橈骨月状骨関節の高さを保持するような形で移植する．内固定としてK鋼線やHerbert screw，ステープルなどを用い術後6週間の外固定を行う(図11-A, B, C)．

RL固定術でもっとも問題となるのは，可動域の減少である．当科で行った13例の術後平均4年の調査では伸展が術前36°から術後27°，屈曲は術前36°から術後26°とおのおの約10°の低下を認めた[6]．また，Stanleyらの術後評価でもexcellentが64%，goodが36%と良好であり，X線像での病期の進行を認めなかった[26]．Darrach手術単独ではX線像での病期の進行を認める例があり，RL固定術の追加はより安定した手関節の獲得と破壊への進行を防ぐ可能性があると思われ，きわめて有用な方法である．したがって，著者は手根中央関節が温存されている場合にはできるだけRL固定術を行うことが可能であるかどうかを検討することにしている．

②全手関節固定術

RA手関節では手根中央関節のみでの関節破壊は痛みの原因となることが少なく，これのみによって全手関節固定術が適応となる場合は少ないと考えられる．全固定術が適応となるのは手根中央関節のみではなく橈骨手根関節の著明な破壊があり，同側の肩，肘，手指の機能が比較的温存されている活動性の高い若年層や，手関節伸筋腱群が断裂した有痛性の高度な屈曲拘縮が存在する場合に限られる．従来は肘関節が強く罹患している場合には手関節の全固定術の適応はないとされていたが，最近，肘関節に対しては人工肘関節置換術などの良好な手術成績が報告されるようになり，必ずしも肘関節の状態は手関節全固定術の禁忌ではなくなっている．また，全手関節固定術により恒久的な無痛性，安定性を有する関節の再建が可能であり，有力な手関節再建術の1つであることは疑いない．

手関節の固定肢位に関しては意見の分かれるところである．著者は背屈・掌屈および橈・尺屈中間位での固定を原則としているが，両側例では片側は中間位で，対側は10-20°程度の掌屈位で固定するのがよいと考えている．

著者はCarrollら[1]の方法に準じて行っている．手根骨背側をリュエルなどで切除し海綿骨を露出したのち，腸骨より皮質海綿骨をウサギの顔のように採型し，両方の耳に該当する部分は第2，3中手骨基部髄腔へ，顔

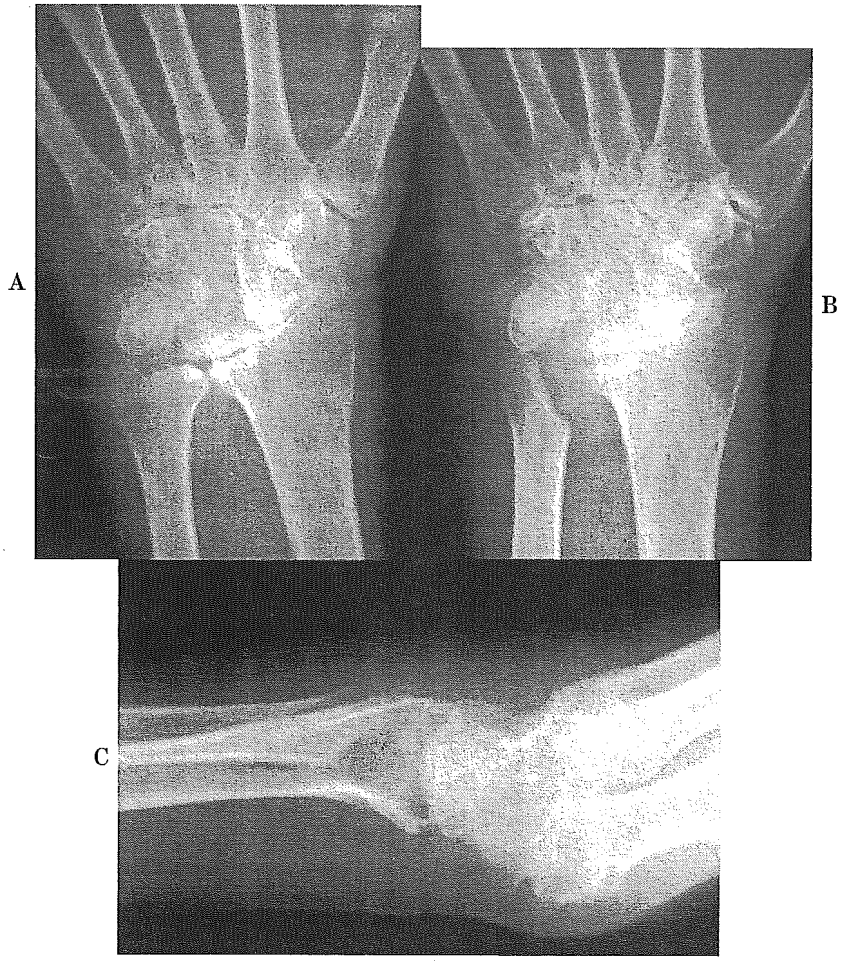

図 10　62 歳女性，左 RA 手関節，stage　IV．(A)術前正面 X 線写真．
(B) Hemiresection-interposition　arthroplasty 後 5 年の正面 X 線写真．
(C) Hemiresection-interposition arthroplasty 後 5 年の側面 X 線写真．

の顎の部分は橈骨遠位髄腔へ挿入する．さらに 2 本の直径 1.8 mm の K 鋼線を腸骨背側で交差させて第 2，3 中手骨と橈骨間を固定する(図 12-A, B, C, D)．これにより移植骨を手根骨に押さえ込むように強固に固定することが可能になる[10),14)]．

③人工手関節置換術

同側の肩，肘，手指の破壊が存在し，手関節の可動域が必要な活動性の低い例が適応となるが，現在のところ長期にわたり安定した成績は残念ながら得られていない．1967 年に Swanson が手関節に関して flexible なシリコン製人工手関節を応用したが，シリコン滑膜炎やインプラントの破損など大きな問題点があった[27)]．1970 年代後半に全人工手関節として Meuli ら[21)]や Volz[32)]などの ball and socket 型人工手関節が開発され臨床応用された．1-2 年の短期成績は良好であったが，5 年前後の長期では遠位コンポーネントのゆるみや脱臼などを生じ failure rate は 30%前後にのぼると報告されている．また，骨切除量が多く，手関節固定術など salvage 手術が困難であることも大きな問題点である．

1983 年から Mayo Clinic で開発され使用されている biaxial wrist prosthesis の 5 年以上の成績では，46 例中 8 例で遠位コンポーネントのゆるみ，1 例で脱臼が生じたとしており，成績は向上していると考えられる[2)]．今後さらに手技および機種の改善による長期成績の向上が望まれる．

RA 手関節の各種手術治療の適応の概略については図 13 に示した．

5. 遠位橈尺関節変形性関節症

遠位橈尺関節(DRUJ)障害を来す代表的疾患として

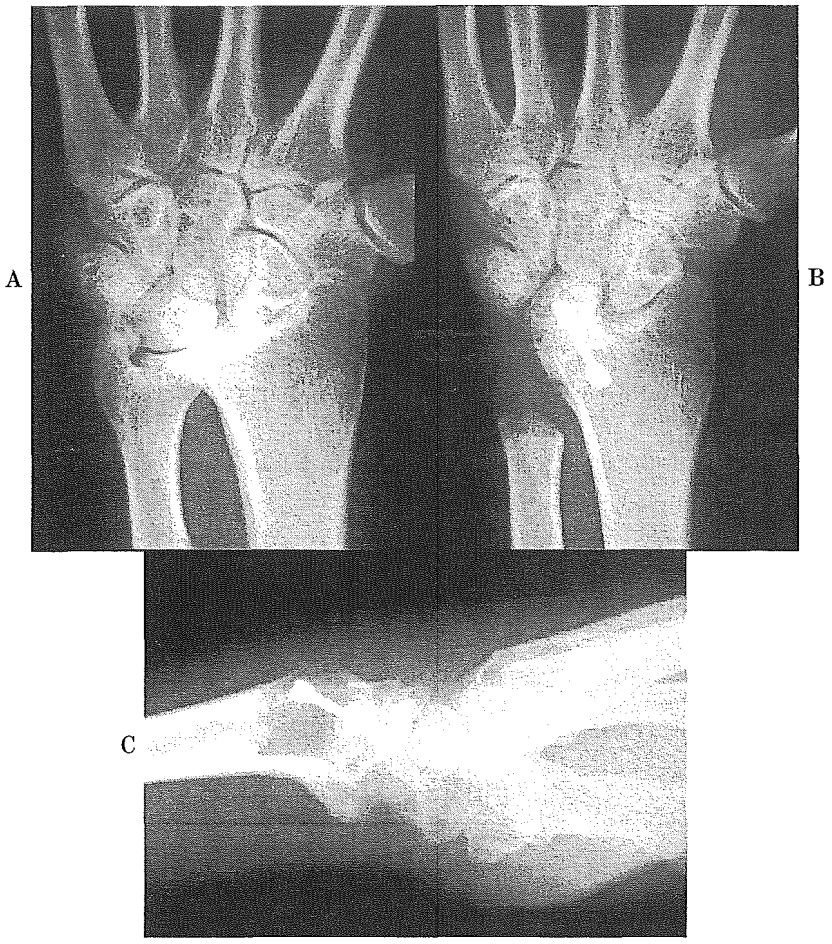

図11 42歳女性，左RA手関節，stage III. (A)術前正面X線写真. (B)橈骨月状骨固定術後4年の正面X線写真. (C)橈骨月状骨固定術後4年の側面X線写真.

は，①DRUJ変形性関節症(DRUJ-OA)，②橈骨遠位端骨折後の変形治癒，③尺骨頭突き上げ症候群，④尺骨茎状突起骨折，⑤尺骨頭(亜)脱臼，⑥TFCC損傷などが存在する．これらのうちDRUJ-OAに関する治療にはさまざまな方法が提唱されているが，保存治療を含め，いまだどの方法がどのような症例に選択されるべきなのかというコンセンサスは得られていない．

1) 保存治療

著者は，DRUJの関節症変化が少なく不安定性が主な原因となっている場合には，手関節を軽度背屈位にしての手関節固定用装具を用いている．本来であれば，DRUJの安定化を図るためには肘上まで含めた長上肢装具とすべきところであるが，肘関節を含めるとADL(activities of daily living)上の不自由度が高くなることもあり，便宜的に短上肢つまり肘下としている．一方，より簡便な方法として尺骨茎状突起から約1 cm遠位から4 cm中枢までに帯状テーピングを行う．つまり尺骨頭を橈骨S状切痕に引き寄せるようにテーピングを行うことにより，不安定性を主訴とした場合には60%程度の効果が得られるとの報告も見られる[20]．著者に経験はないが試みるべき治療手段と考える．

2) 手術療法

先ほども記載したが，DRUJ-OAの病態は多種多様であること，さらにその程度も千差万別というべきであり，これらの複雑な病態を呈するDRUJ-OAに対してどのような手術治療方法を選択すべきであるかについてのコンセンサスは得られていない．ここでは代表的な手術療法について適応を中心に記載する．

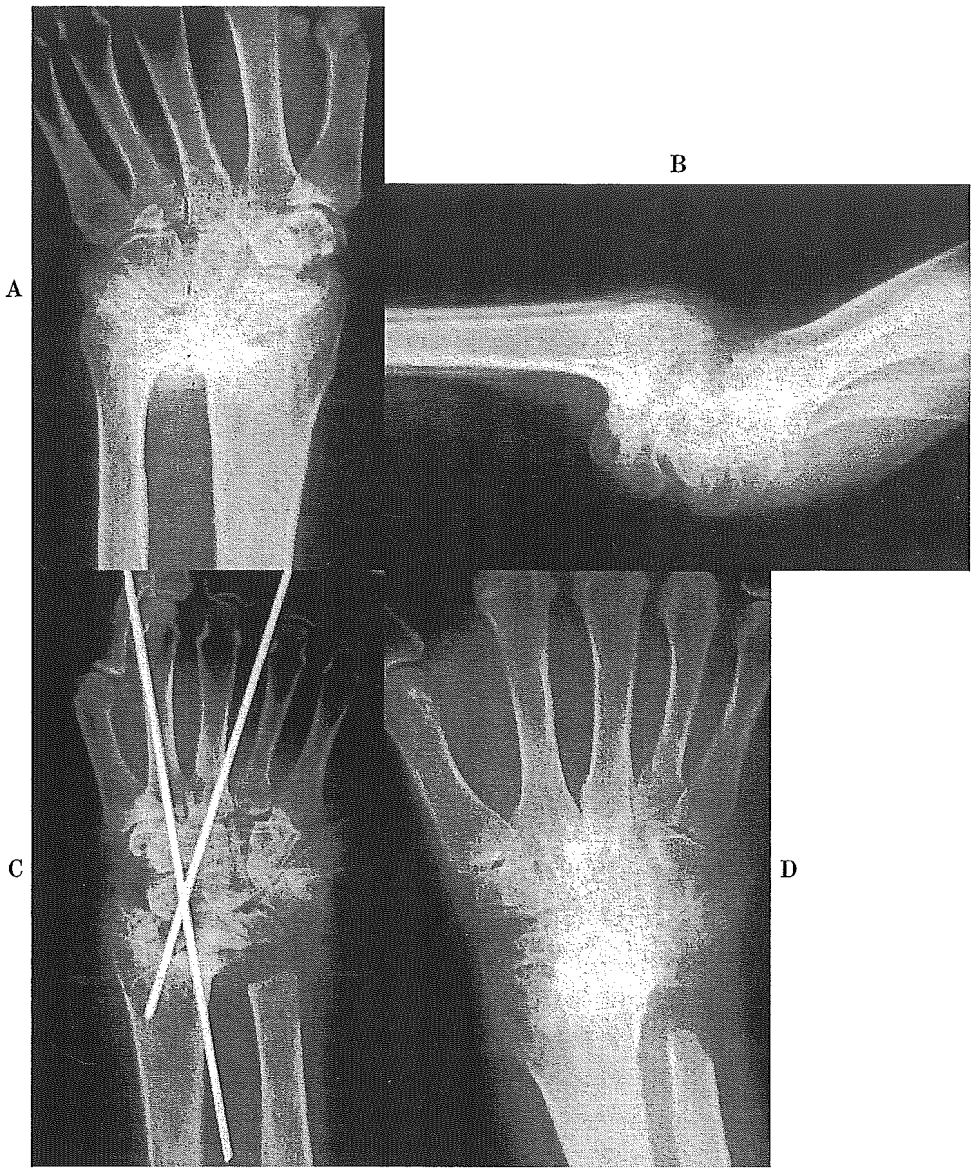

図 12　62 歳女性，右 RA 手関節，stage IV．(A)術前正面 X 線写真．(B)術前側面 X 線写真．(C)腸骨移植および cross bowed K-wire 固定による手関節全固定術を行った直後の正面 X 線写真．(D)腸骨移植および cross bowed K-wire 固定による手関節全固定術を行い 3 年後の正面 X 線写真．

①尺骨短縮術

尺骨がプラスバリアンスを呈している尺骨頭突き上げ症候群が第一義的適応となり得る．しかし，DRUJ-OA の場合，OA の程度が軽症から中等度であることが適応の重要なポイントである．尺骨短縮術は DRUJ-OA に対してはというよりも，TFCC 変性例はもちろんであるが，TFCC 外傷例に対して最近適応が拡大される傾向がある．

しかし，尺骨短縮術による DRUJ の不適合による OA 変化の出現あるいは増悪などの報告も散見され，あまりにも尺骨短縮術が安易に行われている現状に対して著者は警鐘を鳴らしている[12),16),17)]．しかし，尺骨短縮術後の DRUJ-OA の発生に関しては X 線学的な OA 変化と症状が必ずしも一致しないことが多いために，DRUJ の不適合というよりは adaptation つまり適応していると考えるべきとの考えもある．これらについては今後の検討課題であろう．

皮切は尺側手根屈筋(flexor carpi ulnaris: FCU)腱および ECU 腱の間で遠位尺骨の骨稜を触れる部位に縦切開を加える．著者は原則として 6 穴の小型 dynamic

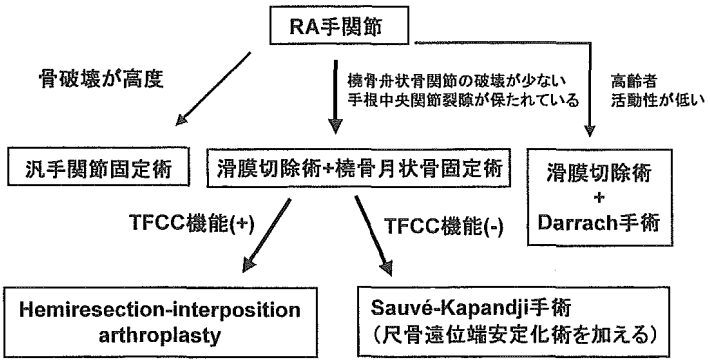

図 13　RA 手関節の手術治療体系.

compression plate (DCP) を用いているので，その最遠位が尺骨の茎状突起よりも 1-2 cm 近位が皮切の遠位部ということになる．小型 DCP は内固定材料として容量がかなり大きいので骨癒合後，抜釘を必要とする場合が多い．また骨切り部の骨癒合が primary healing し，仮骨形成が少ないなどの理由により嫌う報告も散見されるが，著者は術後外固定をしないで済むなどより好んで用いている．少し掌側よりに皮切を移動してプレートを FCU の筋肉でカバーするような工夫も試みている．尺骨の尺側縁の骨稜の骨膜を縦切して尺骨を露出する．プレートをあてて骨切り部を同定し，あらかじめ決定した尺骨短縮量の骨切除を行う．著者は単純な cylindrical な骨切除を行っているが，尺骨は骨皮質が厚く骨髄腔が狭く，遷延治癒あるいは偽関節などの報告が多い理由により，step-cut osteotomy など，骨の接触面積を多くする試みなどもなされている．

短縮 (切除) 量については，従来は尺骨バリアンス“O”を目指していたが，その必要性についてはまだ一定の見解が得られていない．著者の経験では短縮量が多いと術後の DRUJ-OA の発生率が高い傾向にあることを認めている．したがって最近では尺骨のバリアンスというよりも 2 mm 程度の短縮で十分ではないかと考えている．この点についてはいまだコンセンサスは得られていない．

短縮する前にまず，プレートを当ててもっとも遠位の hole に screw を途中まで刺入して，回旋を防ぐためのメルクマールを骨切り部の尺骨の近位と遠位に印した後にサジタルプレーンソーを用いて骨切りを行い，手関節を尺屈位にして回旋に注意してプレートを戻して 6 本すべての screw 刺入を行う．わずかな回旋の相違は許容できるものと考える．固定性が良好であることを確認後，可及的に骨膜でプレートを被覆することにする[7),12)].

抜糸までの期間は創の安静と疼痛の軽減のために前腕以降のギプス副子固定を行うが，その後は自由な運動を許可している．しかし，骨癒合が完全に得られるまでは重量物の挙上や contact sports などは禁止する．

②Sauvé-Kapandji 法[15)–17),19)]

Sauvé-Kapandji (S-K) 法の最も良い適応は DRUJ の一次性変形性関節症である．ただし，DRUJ-OA の場合で TFCC の機能が消失しており，かつ TFCC 機能の再建ができない場合が適応と考えている．S-K 法は最近最も多く行われている手術である．手技については RA 手関節の項で記載したのでここでは割愛する．

③Hemiresection-interposition arthroplasty[11),13),16)–18)]

Hemiresection-interposition arthroplasty (HIA) は前にも記載しているが Bowers らがはじめて提唱したものである．橈骨の尺骨切痕に対応するように尺骨頭を形成するものである．著者は TFCC が機能している，あるいは TFCC の機能を再建できる場合の DRUJ-OA に適応があると考えている．簡単に言うと TFCC の損傷の程度が軽度であれば HIA を，程度が強ければ S-K 法を行うこととしている．したがって頻度的には HIA よりも S-K 法を行うことの方がどうしても多くなる．手術手技については RA 手関節の項で記載したのでここでは割愛する．

④Darrach 手術

尺骨遠位端を切除する Darrach 手術は S-K 手術および HIA などが導入される前にはどのような原因による DRUJ 障害に対しても，もっぱら行われていた．しか

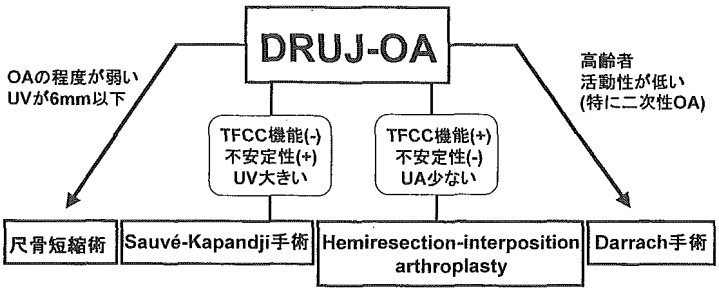

図 14　遠位橈尺関節変形性関節症に対する手術治療体系.

し，Darrach 手術後に握力の低下や尺骨遠位端の不安定性などの合併症が高率に発生することが認識され，最近ではあまり用いられていないのが現状である[16),17)]．しかし，関節リウマチ患者あるいは高齢者で活動性の低い患者などの DRUJ 障害に対しては今でも広く用いられている．橈骨遠位端骨折が高齢者に発生することが多いこともあり，二次性 DRUJ-OA などは本法が適応となることが多い．手術手技については RA 手関節の項で記載しているのでここでは割愛する．

最後に，著者の考えている DRUJ-OA に対する手術治療の治療手段についてアルゴリズムを図 14 に示す．

本研究の施行にあたり加藤博之教授(信州大学)，北海道大学病院および北海道大学関連病院の先生方に多大なご協力をいただきました．ここに深く感謝申し上げます．

文　　献

1) Carroll RE, Dick HM. Arthrodesis of the wrist for rheumatoid arthritis. J Bone Joint Surg Am 1971; 53: 1365-9.
2) Cobb TC, Beckenbaugh RD. Biaxial total-wrist arthroplasty. J Hand Surg Am 1996; 21: 1011-5.
3) Ford DJ, Khoury G, el-Hadidi S, et al. The Herbert screw for fractures of the scaphoid. A review of results and technical difficulties. J Bone Joint Surg Br 1987; 69: 124-7.
4) Herbert TJ, Fisher WE. Management of the fractured scaphoid using a new bone screw. J Bone Joint Surg Br 1984; 66: 114-23.
5) 石川淳一，三浪明男，岩崎倫政．RA 手関節の手術．整・災外 2004; 47: 733-40.
6) 岩崎倫政，三浪明男，加藤博之他．慢性関節リウマチ手関節に対する橈骨月状骨間固定術の術後成績—Darrach 法単独群と比較して—．日手会誌 1999; 16: 183-6.
7) 加藤博之，三浪明男，笠島俊彦．TFCC 損傷に対する尺骨短縮術．別冊整形外科 1997; 31: 131-3.
8) Mayfield JK, Johnson RP, Kilcoyne RF. The ligaments of human wrist and their functional significance. Anat Res 1976; 186: 417-28.
9) 三浪明男．三角線維軟骨複合体(TFCC)総論．整・災外 1996; 39: 1409-16.
10) 三浪明男．手関節固定術における術式の工夫—確実な骨癒合を得るために—．MB Orthop 2000; 13: 30-4.
11) Minami A, Kaneda K, Itoga H. Hemiresection-interposition arthroplasty of the distal radioulnar joint associated with repair of triangular fibrocartilage complex lesion. J Hand Surg Am 1991; 16: 1120-4.
12) Minami A, Kato H. Ulnar shortening for triangular fibrocartilaginous complex. J Hand Surg Am 1990; 15: 415-20.
13) 三浪明男，石川淳一．リウマチ患者の上肢機能障害—評価と治療．手関節機能再建術の適応と実際．リウマチ科 2004; 32: 477-85.
14) Minami A, Kato H, Iwasaki N. Total wrist arthrodesis using bowed crossed K wires. J Hand Surg Br 1999; 24: 410-4.
15) Minami A, Kato H, Iwasaki N. Modification of the Sauvé-Kapandji procedure with extensor carpi ulnaris tenodesis. J Hand Surg Am 2000; 25: 1080-3.
16) 三浪明男，萩野利彦，福田公孝他．遠位橈尺関節障害に対する治療法の検討．日手会誌 1986; 3: 530-3.
17) Minami A, Ogino T, Minami M. Treatment of distal radioulnar disorders. J Hand Surg Am 1987; 12: 189-96.
18) Minami A, Suzuki K, Suenaga N, et al. Hemiresection-interposition arthroplasty for osteoarthritis of the distal radioulnar joint. Int Orthop 1995; 19: 35-9.
19) Minami A, Suzuki K, Suenaga N, et al. The Sauvé-Kapandji procedure for osteoarthritis of the distal radioulnar joint. J Hand Surg Am

1995; 20: 602-8.
20) 水関隆也. TFCC損傷の治療法—保存療法を中心として—. 関節外科 1994; 13: 986-94.
21) Mueli HC, Fernandez DC. Uncemented total wrist arthroplasty. J Hand Surg Am 1995; 20: 115-20.
22) 小川亮恵, 南川義隆. RAの手関節, 指関節の滑膜切除術適応, 手技と長期成績. 関節外科 1993; 12: 25-31.
23) Palmer AK, Werner FW. The triangular fibrocartilage complex of the wrist-anatomy and function. J Hand Surg Am 1981; 6: 153-62.
24) 佐々木孝. 舟状骨骨折に対する治療法の選択. MB Orthop 1989; 13: 19-25.
25) Slade JF, Gutow AP, Geissler WB. Percutaneous internal fixation of scaphoid fractures via an arthroscopically assisted dorsal approach. J Bone Joint Surg Am 2002; 84: 21-36.
26) Stanley JK, Tolat AR. Long-term results of Swanson silastic arthroplasty in the rheumatoid wrist. J Hand Surg Br 1993; 18: 381-5.
27) Swanson AB. Flexible implant arthroplasty for arthritic disabilities of the radiocarpal joint. Orthop Clin North Am 1973; 4: 383-90.
28) Taleisnik J. The ligaments of the wrist. J Hand Surg 1976; 1: 110-8.
29) 田中寿一, 柳田博美, 大迎知宏他. 舟状骨骨折に関する新しいscrew(DTJ)の開発と治療. 日手会誌 2002; 19: 643-7.
30) 藤哲. Herbert screwによる手舟状骨骨折治療. MB Orthop 1989; 13: 27-35.
31) 坪川直人, 吉津孝衛, 牧裕. 舟状骨骨折の小皮切による刺入固定. 整・災外 2001; 44: 1359-67.
32) Volz RG. The development of a total wrist arthroplasty. Clin Orthop 1976; 116: 209-14.
33) Watson HK, Ballet FL. The SLAC wrist: scapholunate advanced collapse pattern of degenerative arthritis. J Hand Surg Am 1984; 9: 758-65.

Available online at www.sciencedirect.com
SCIENCE DIRECT®
Analytical Biochemistry 339 (2005) 69–72
ANALYTICAL BIOCHEMISTRY
www.elsevier.com/locate/yabio

Carbohydrate analysis by a phenol–sulfuric acid method in microplate format

Tatsuya Masuko[a,b,c,*], Akio Minami[b], Norimasa Iwasaki[b], Tokifumi Majima[b], Shin-Ichiro Nishimura[c], Yuan C. Lee[a]

[a] *Department of Biology, Johns Hopkins University, 3400 North Charles Street, Baltimore, MD 21218, USA*
[b] *Department of Orthopaedic Surgery, Hokkaido University School of Medicine, Kita-15, Nishi-7, Kita-Ku, Sapporo 060-8638, Japan*
[c] *Laboratory for Bio-Macromolecular Chemistry, Division of Biological Sciences, Graduate School of Science, Frontier Research Center for the Post-Genomic Science and Technology, Hokkaido University, Kita-21, Nishi-11, Kita-Ku, Sapporo 001-0021, Japan*

Received 18 October 2004
Available online 27 December 2004

Abstract

Among many colorimetric methods for carbohydrate analysis, the phenol–sulfuric acid method is the easiest and most reliable method. It has been used for measuring neutral sugars in oligosaccharides, proteoglycans, glycoproteins, and glycolipids. This method is used widely because of its sensitivity and simplicity. In its original form, it required 50–450 nmol of monosaccharides or equivalent for analysis and thus is inadequate for precious samples. A scaled-down version requiring only 10–80 nmol of sugars was reported previously. We have now modified and optimized this method to use 96-well microplates for high throughput, to gain greater sensitivity, and to economize the reagents. This modified and optimized method allows longer linear range (1–150 nmol for Man) and excellent sensitivity. Moreover, our method is more convenient, requiring neither shaking nor covering, and takes less than 15 min to complete. The speed and simplicity of this method would make it most suitable for analyses of large numbers of samples such as chromatographic fractions.

Keywords: Carbohydrate; Analysis; Phenol; Sulfuric acid; Microplate

Measurement of carbohydrate contents in a variety of samples is a basic analytical operation in many phases of biosciences. Among many colorimetric methods for carbohydrate determination, the phenol–sulfuric acid method [1,2] is the easiest and most reliable method for measuring neutral sugars in oligosaccharides, proteoglycans, glycoproteins, and glycolipids. The phenol–sulfuric acid method is used widely because of its sensitivity and simplicity. Other methods using anthrone [3], orcinol [4], or resorcinol [5] may be as sensitive but are not as convenient. In its original form [2], it required 50–450 nmol of monosaccharides or equivalent for analysis and thus is inadequate for precious samples. A scaled-down version of it requiring only 10–80 nmol of sugars was developed before [6]. We have now adapted this method for 96-well microplates for higher throughput to gain greater sensitivity and to economize the reagents. Monsigny et al. [5] reported a resorcinol–sulfuric acid assay in microplate format, but it needed covering the reaction mixture with a layer of pristane, vortexing, and heating at 90 °C in an oven for 30 min. Recently, Laurentin and Edwards [3] reported a microplate version of the anthrone method which also required covering of the wells with clingfilm and acetate tape, vortexing twice, incubating at 92 °C in a nonshaking water bath, and additional drying in an oven at

* Corresponding author. Fax: +1 410 516 8716.
E-mail address: masuko@med.hokudai.ac.jp (T. Masuko).

0003-2697/$ - see front matter © 2004 Elsevier Inc. All rights reserved.
doi:10.1016/j.ab.2004.12.001

45 °C for 15 min. In this paper, we report a simpler and more sensitive phenol–sulfuric acid assay using a 96-well microplate, without additional shaking or drying of the plate.

Materials and methods

Materials

Concentrated sulfuric acid and phenol were from J.T. Baker (Phillipsburg, NJ). D-Mannose (Man), D-xylose (Xyl), L-fucose (Fuc), D-galactose (Gal), and D-glucosamine hydrochloride (GlcN) were from Pfanstiehl Laboratories, Inc. (Waukegan, IL). L-Glucose (Glc), D-galacturonic acid (GalUA), and *N*-acetylneuraminic acid (NeuAc) were from Sigma Chemical Co. (St. Louis, MO). A 96-well, flat-bottomed, polystyrene miocroplate (Nunc, Cat. No. 269620) was from VWR (Bridgeport, NJ). A microplate shaker (Model Titer plate shaker) was from Lab-Line Instruments Inc. (Melrose Park, IL). A spectrophotometer (Model UV 160) was from Shimadzu Scientific Instruments, Inc. (Columbia, MD). A microplate reader (Model Benchmark) and its accompanying software, Microplate Manager, version 5.1, were from Bio-Rad Laboratories (Richmond, CA). All regression analyses were performed with a software Prism (GraphPad Software, San Diego, CA).

Optimization of microplate-based method

Rao and Pattabiraman [7] reported that, in the phenol–sulfuric acid reaction, phenol underwent sulfonation in situ and the phenol–sulfonic acid formed decreased the color intensity for many hexoses and pentoses. Similarly, our preliminary experiments indicated that the addition of concentrated sulfuric acid to the sample followed by phenol (abbreviated sulfuric acid–phenol) yielded the best results. This protocol was optimized for shaking time and volumes of sulfuric acid and phenol as described below.

Shaking time. To 50 µl of Man in a well (100 nmol/well) of a 96-well microplate was added rapidly 150 µl of concentrated sulfuric acid and the mixture was shaken for 0–30 min. Then, 30 µl of 5% phenol in water was added and the mixture was heated for 5 min at 90 °C in a static water bath (the microplate was carefully floated). After cooling to room temperature for 5 min in another water bath, the microplate was wiped dry and $A_{490\ nm}$ was measured by microplate reader.

Volume of concentrated sulfuric acid. To 50 µl of Man in a well (100 nmol/well) of a 96-well microplate was added 0–150 µl of concentrated sulfuric acid rapidly. Immediately thereafter, 30 µl of 5% phenol was added and the plate was kept in a static water bath for 5 min at 90 °C. After cooling to room temperature for 5 min in another water bath, it was wiped dry and $A_{490\ nm}$ was measured by microplate reader.

Volume of 5% phenol. To 50 µl of Man in a well (100 nmol/well) of a 96-well microplate was added 150 µl of concentrated sulfuric acid as above, followed immediately with 0–100 µl of 5% phenol. The plate was heated for 5 min at 90 °C as above. After cooling to room temperature for 5 min in another water bath, it was wiped dry and $A_{490\ nm}$ was measured.

Results

Optimization of reaction conditions

For survey of optimal reaction conditions, we considered five factors, including sample size, sequence of addition, shaking time between additions of concentrated sulfuric acid and phenol, amount of concentrated sulfuric acid, and amount of 5% phenol. We selected the sample size of 50 µl to allow addition of sufficient amounts of sulfuric acid and the phenol solutions. Of the three sequences tested, sample–phenol–sulfuric acid and phenol–sulfuric acid–sample had lower absorbances than sample–sulfuric acid–phenol, and therefore the last sequence was adopted. Using this sequence, and when the 5% phenol was added immediately after the concentrated sulfuric acid, the maximal absorbance was obtained (Fig. 1).

It appears that the maximal absorbance was obtained when 150 µl of concentrated sulfuric acid and 30 µl of 5% phenol were added in rapid succession to 50 µl of Man (Figs. 2A and B).

Final optimized microplate phenol–sulfuric acid assay

To 50 µl of Man in a well (100 nmol/well) of a 96-well microplate was added 150 µl of concentrated sulfuric

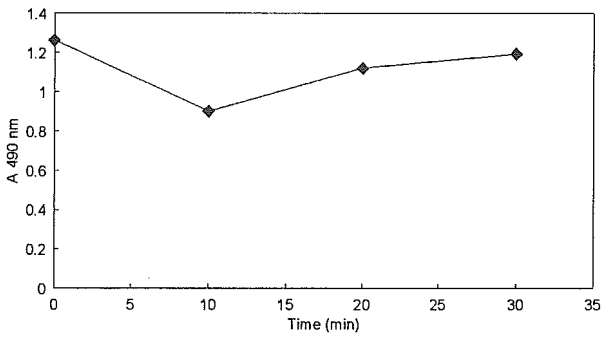

Fig. 1. Effect of the addition of 5% phenol at different time intervals after addition of concentrated sulfuric acid on the absorbance at 490 nm.

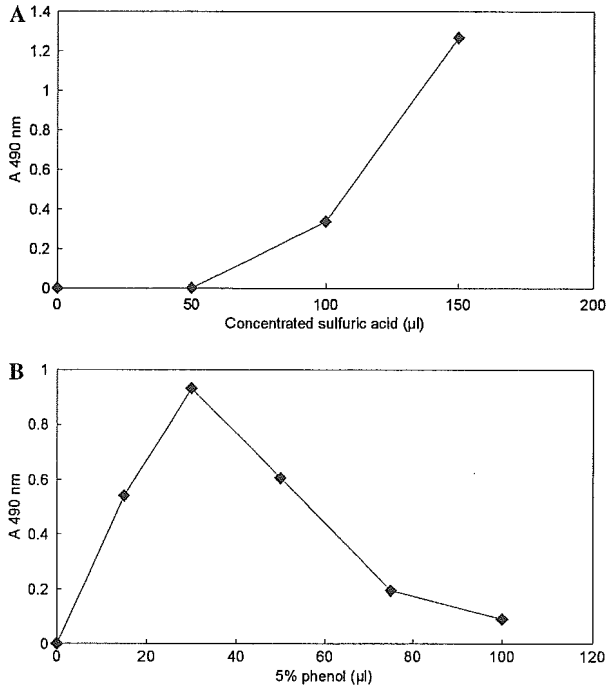

Fig. 2. (A) Influence of the volume of concentrated sulfuric acid on the absorbance at 490 nm. (B) Influence of the volume of 5% phenol on the absorbance at 490 nm.

acid rapidly to cause maximum mixing, followed immediately by 30 μl of 5% phenol in water. After incubating for 5 min at 90 °C in a static water bath by floating the microplate carefully, the plate was cooled to room temperature for 5 min in another water bath and wiped dry to measure $A_{490\ nm}$ by microplate reader. The whole assay takes <15 min.

Relative absorbance

Eight sugars (Man, Xyl, Fuc, Gal, Glc, GlcN, GalUA, and NeuAc) were individually evaluated by this optimized microplate assay. Table 1 shows that each sugar (100 nmol/well) had different absorbance and relative absorbance at 490 nm. The absorbance of Xyl was the highest, but that of GlcN was negligibly low, as expected.

Table 1
Color responses of different sugars ($n = 5$)

Sugar	Absorbance (at 490 nm)	Relative absorbance[a]
Man	1.259	100
Xyl	2.098	167
Fuc	1.103	88
Gal	1.178	94
Glc	1.482	118
GlcN	0.039	3
GalUA	0.832	66
NeuAc	0.030	<3

[a] Relative absorbance is the number based on the absorbance obtained with Man as 100.

Absorption spectra

Five sugars (Man, Xyl, Fuc, Gal, and Glc) for spectral measurement were generated by this optimized assay. Five wells (100 nmol/well) were used for each sugar. After incubating and cooling to room temperature, the products in five wells were put together and applied to one cuvette to measure by spectrophotometer. Fig. 3 shows that at 490 nm most sugars can be measured at or near their absorption maxima and that the absorption spectra of Man, Xyl, Fuc, Gal, and Glc have peaks at 491, 486, 482, 491, and 493 nm, respectively.

Linearity of color responses

A linear relationship between the absorbance and the sugar quantity was observed within the range of 1–150 nmol/well of Man. Figs. 4A–C show the regression

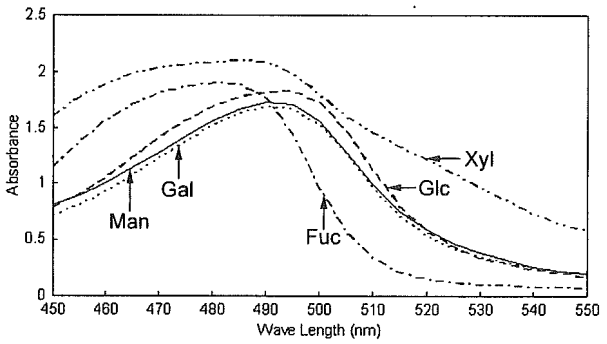

Fig. 3. Absorption spectra of color products from of Man, Xyl, Fuc, Gal, and Glc. Peaks are at 491, 486, 482, 491, and 493 nm, respectively.

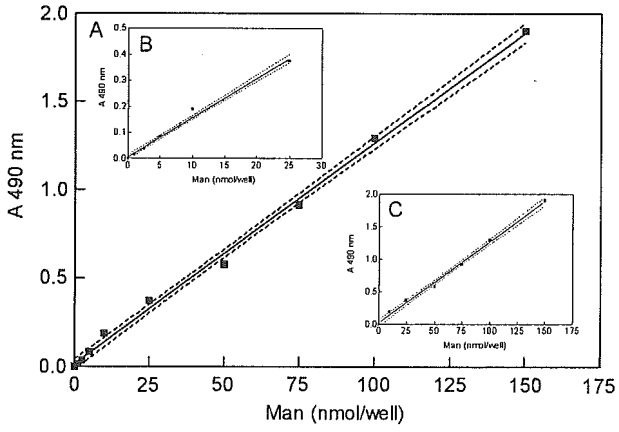

Fig. 4. Lines of Man within 1–150 nmol/well (A), 1–25 nmol/well (B), and 10–150 nmol/well (C) on the absorbance at 490 nm.

Table 2
Linearity of color responses ($n = 4$)

Range (nmol/well)	Regression equation	Coefficient of determination $(r^2)^2$	Standard deviation
1–150	$\hat{Y} = 0.01251X + 0.01390$	0.9880	0.07016
1–25	$\hat{Y} = 0.01511X + 0.005961$	0.9868	0.01638
10–150	$\hat{Y} = 0.01247X + 0.01823$	0.9834	0.08382

Table 3
Comparison of microplate versions of phenol–sulfuric acid method

Authors	Coloring reagent	Detectable range (nmol/well)	Shake times	Requirements
Monsigny et al. [5]	Resorcinol	1–20 (at 430 nm) 10–100 (at 480 nm)	Once	Pristane
Laurentin and Edwards [3]	Anthrone	11.1–88.8	Twice	Clingfilm Acetate tape
This report	Phenol	1–150	No time	None

lines within 1–150 nmol/well, 1–25 nmol/well, and 10–150 nmol/well, respectively. Table 2 shows their constants, coefficient of determinations $(r^2)^2$, and estimated standard deviations (s).

Discussion

Table 3 shows comparison of our method with two previous reports using microplates. Monsigny et al. [5] and Laurentin and Edwards [3] reported microplate assays using resorcinol and anthrone, respectively, but both requiring shaking and adding of pristane to avoid any projection or covering of the plate or plate wells.

In addition to not requiring the cumbersome covering and shaking, our method has many advantages: (1) it requires less than 15 min (2) it requires only small amounts of phenol and sulfuric acid and (3) it is quite sensitive with a workable range of 1–150 nmol/well.

The speed and simplicity of this method would make it most suitable for high-throughput analyses of large number of samples such as chromatographic fractions with little consumption of materials.

References

[1] M. Dubois, K. Gilles, J.K. Hamilton, P.A. Rebers, F. Smith, A colorimetric method for the determination of sugars, Nature 168 (1951) 167.
[2] M. Dubois, K.A. Gilles, J.K. Hamilton, P.A. Rebers, F. Smith, Colorimetric method for determination of sugars and related substances, Anal. Chem. 28 (1956) 350–356.
[3] A. Laurentin, C.A. Edwards, A microtiter modification of the anthrone–sulfuric acid colorimetric assay for glucose-based carbohydrates, Anal. Biochem. 315 (2003) 143–145.
[4] M. Irwin, A.G. Leaver, Use of the orcinol–sulphuric acid reaction in the positive identification of certain monosaccharides from a salivary mucoid, Nature 177 (1956) 1126.
[5] M. Monsigny, C. Petit, A.C. Roche, Colorimetric determination of neutral sugars by a resorcinol sulfuric acid micromethod, Anal. Biochem. 175 (1988) 525–530.
[6] Y.C. Lee, J.F. McKelvy, D. Lang, Rapid automatic analysis of sugar components of glycoproteins. II. Neutral sugars, Anal. Biochem. 27 (1969) 567–574.
[7] P. Rao, T.N. Pattabiraman, Reevaluation of the phenol–sulfuric acid reaction for the estimation of hexoses and pentoses, Anal. Biochem. 181 (1989) 18–22.

Thiolation of Chitosan. Attachment of Proteins via Thioether Formation

Tatsuya Masuko,[†,‡,§] Akio Minami,[‡] Norimasa Iwasaki,[‡] Tokifumi Majima,[‡] Shin-Ichiro Nishimura,[§] and Yuan C. Lee*[,†]

Department of Biology, Johns Hopkins University, 3400 North Charles Street, Baltimore, Maryland 21218, Department of Orthopaedic Surgery, Hokkaido University School of Medicine, Kita-15, Nishi-7, Kita-Ku, Sapporo 060-8638, Japan, and Laboratory for Bio-Macromolecular Chemistry, Division of Biological Sciences, Graduate School of Science, Frontier Research Center for the Post-Genomic Science and Technology, Hokkaido University, Kita-21, Nishi-11, Kita-Ku, Sapporo 001-0021, Japan

Received October 14, 2004; Revised Manuscript Received December 1, 2004

Chitosan has a variety of biological functions through conjugating of other compounds to their amino and hydroxyl groups. To further expand applicability of chitosan, we have modified the amino group of chitosan with 2-iminothiolane to bestow thiol groups and obtained about 20% yield, which is equivalent to 913 μequiv SH/g chitosan or 457 nequiv SH/nmol chitosan. Bovine serum albumin (BSA) was reacted with *N*-(ϵ-maleimidocaproyloxy)sulfosuccinimide ester (sulfo-EMCS), and maleimide-modified BSA (MalN-BSA) was obtained. The yield of sulfo-EMCS addition was 12.8−36.8 mol MalN/mol BSA. When the chitosan-SH was reacted with MalN-BSA via thioether, 97.8% of the maleimide group was reacted, and 37.2% of the SH group was consumed. The remaining SH group was quenched by bromoacetamide. This is the first report of covalent conjugation of a protein to chitosan. Our method should find many applications in developing new chitosan-based biomedical materials containing other components such as growth factors and cell adhesion molecules, known to be crucial to cells. Our thiolated chitosan will facilitate conjugation of such biomedical components to provide new types of materials for tissue engineering.

Introduction

Chitin [poly-β-(1→4)-*N*-acetyl-D-glucosamine] is an ubiquitous biopolymer found in the exoskeleton of insects and marine invertebrates and is the second most abundant biomaterial. Chitosan is a poly-β-(1→4)-D-glucosamine and is prepared by de-*N*-acetylation of chitin. Chitosan is also naturally present in some microorganisms and fungi. Although chitosan is insoluble in neutral or alkaline aqueous solution, it dissolves in dilute acid solutions, such as hydrochloric, lactic, and acetic acid.[1]

Chitosan and its derivatives are found to have antimicrobial, antifungal, antiviral,[2] and anticholesteremic activities,[3,4] and they are also known to activate biological defense mechanisms. For example, chitosan (ca. 70% de-*N*-acetylated) showed macrophage activation, cytokine production, and antiinfectious activity.[5]

Availability of numerous amino and hydroxyl groups allows chitosan to be conjugated with antiviral,[6] antimicrobial,[7] antitumor,[8,9] and anticoagulant[10] agents, as well as peptides,[11] collagen,[12] and fluorescent compounds.[13−16] Moreover, chitosan has been used as a drug delivery system for proteins,[17−19] growth factors,[19−22] DNA,[23−27] anticancer drugs,[9,28−31] taurine,[32] and insulin.[33] Chitosan can be fabricated into films,[21,22,34−40] fibers,[21,41,42] sponges,[20,43] porous scaffolds,[12,44−46] gels,[19,32,47−50] tubes,[11] microspheres,[21,28,30] microcapsules,[33] and nanoparticles.[14,17,18,25,31]

Chitosan is reported to be biocompatible,[24,35,37,43,48,51] biodegradable,[15,28,35,43,52] and of low toxicity.[9] Chitosan is degraded by lysozyme, and the degradation is slower, both in vitro and in vivo, for more highly deacetylation samples.[15,35,52−54]

The cytotoxicity of chitosan is reported to be dose-dependent and decreases with a decrease in molecular weights and degrees of de-*N*-acetylation.[55] However, chitosan of 700 kDa or larger has been used safely in actual clinical applications.[43,48,56] Additionally, chitosan has partial structural similarities to glycosaminoglycans, which are essential structural elements of the extracellular matrix of most tissues. Therefore, chitosan and its derivatives have been investigated as tissue engineering scaffold for bone,[20,37] liver,[21,34,40] nerve,[11] cartilage,[37−39,41,42,45−47] and skin.[12,32,36,50,57] Chitosan has been reported to accelerate early phase healing of open skin wounds by increasing the rate of infiltration of polymorphonuclear cells and the production of collagen by fibroblasts.[58] In fact, chitosan is a component in a commercial product, Tegasorb,[1] which is used as wound dressings for dermal ulcers and skin tears. *N*-Carboxybutyl chitosan was applied to four patients undergoing plastic surgery.[56] Chitosan and methylpyrrolidinone chitosan also have been used for the treatment of periodontitis[48] and dysodontiasis,[43] respectively.

* To whom correspondence should be addressed. Tel.: 1-410-516-7041. Fax: 1-410-516-8716. E-mail: yclee@jhu.edu.
† Johns Hopkins University.
‡ Hokkaido University School of Medicine.
§ Hokkaido University.

10.1021/bm049352e CCC: $30.25
Published on Web 02/08/2005

We have modified the amino group of chitosan with 2-iminothiolane to bestow thiol groups and obtained about 20% to which maleimide-modified bovine serum albumin (MalN-BSA) was conjugated via thioether in high yield. BSA, a commonly accepted standard protein, was selected as a model protein to be conjugated to thiolated chitosans preparatory to conjugation of growth factors and cell adhesion molecules. Our thiolated chitosan will facilitate conjugation of such biomedical components to provide new types of materials for tissue engineering.

Materials and Methods

Materials. Chitosan (ca. 500 kDa, ca. 80% deacetylated) was from Yaizu Suisankagaku Industry Co. (Yaizu-City, Japan). Bromoacetamide and 2-iminothiolane were from Aldrich Chemical Co. (Milwaukee, WI). Dithiothreitol (DTT), Ellman's reagent [5,5′-dithio-bis-(2-nitrobenzoic acid), DTNB], and L-cysteine were from Sigma Chemical Co. (St. Louis, MO). Sepharose CL-6B and Sephadex G-50 were from Amersham (Piscataway, NJ). Nunc microplates of 96 flat-bottom wells (catalog no. 269620) were from Fisher Scientific (Pittsburgh, PA). Sulfo-EMCS [*N*-(ϵ-maleimidocaproyloxy)sulfosuccinimide ester] and MalNEt (*N*-ethylmaleimide) were from Pierce (Rockford, IL). BSA was from Bayer (Kankakee, IL).

Buffers and Columns. Buffer A consisted of 50 mM potassium phosphate (pH 6.0), 150 mM NaCl, and 2 mM ethylenediaminetetraacetic acid. Buffers B and C consisted of the same components as buffer A, but the pH was adjusted to 7.0 and 8.0, respectively.

Unless otherwise mentioned, a Sepharose CL-6B column (1 × 24 cm) in buffer B was used to isolate thiolated chitosan derivatives, collecting 1.6-mL fractions at 0.6 mL/min. The effluent was monitored with $A_{245\ nm}$ by a flow monitor (model V^4) from ISCO (Lincoln, NE) and with the Ellman's method for thiol content.[59]

Instrumentation. A microplate reader (model Benchmark) and its accompanying software, Microplate Manager, version 5.1, were from Bio-Rad Laboratories (Richmond, CA). A spectrophotometer (model UV 160) was from Shimadzu Scientific Instruments, Inc. (Columbia, MD).

Graphic Presentation and Regression Analyses. All graphic presentation and regression analyses were performed with a graphing software Prism (GraphPad Software, San Diego, CA).

Ellman's Method for Thiol Group Analysis. Samples (100 μL) were placed in the wells of a 96-well microplate and mixed with 50 μL of 0.1 M borate buffer (pH 8.0) and 10 μL of DTNB solution. After 15 min, the developed color was measured at 415 nm. A standard curve was constructed in parallel using cysteine and analyzed by linear regression with Prism.

Optimization of the Reaction of Chitosan with 2-Iminothiolane. Reaction of 2-iminothiolane with amino groups bestows SH groups to chitosan while retaining the positive charge of the NH_2 groups. The 2-iminothiolane reaction optimized with respect to pH, reaction time, and temperature was carried out.

Scheme 1. Chitosan Reacting with 2-Iminothiolane To Yield Chitosan-SH

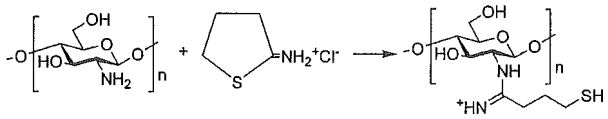

(I) Reaction pH. Chitosan (60 mg) was suspended in 10 mL each of buffer A, B, or C. One hundred microliters each of these chitosan suspensions was mixed with 25 mg of 2-iminothiolane and 400 μL of 2% DTT, and the mixture was agitated at 60 °C for 6 h. Although the chitosan became soluble only when buffer A (pH 6.0) or B (pH 7.0) was used (Scheme 1), the thiolation yield using buffer A (3.5%) was lower than that using buffer B (19.0%). The chitosan became turbid and never clarified during the thiolation reaction when buffer C (pH 8.0) was used. Therefore, buffer B (pH 7.0) was selected as the reaction buffer throughout this paper.

(II) Reaction Temperature. The optimal temperature for thiolation was examined in the temperature range of 45−65 °C, and the reaction mixture was kept for 7 h.

(III) Reaction Time. The optimal reaction time was examined at 60 °C from 4 to 10 h. The reaction mixture became soluble and remained soluble even after 10 h.

(IV) Turbidity. To evaluate solubilization during the reaction from 0 to 4 h, the turbidity was measured by $A_{650\ nm}$. Briefly, the absorbance at 650 nm was measured on a spectrophotometer after 1 mL of sample was reacted for 0, 1, 2, 3, and 4 h.

Solubility of Unmodified Chitosan. The solubility of chitosan at different pH values was examined. Chitosan powder (4 g) was mixed with 1% acetic acid (200 mL) to make a 2% (w/v) stock chitosan solution (pH 2.68). To 2.0 mL of the chitosan stock solution were added suitable amounts of 0.2 M borate buffer (pH 10.0) to adjust the pH to 3.0, 4.0, 5.0, or 6.0. After standing at 20−22 °C for 1 h, the turbidity was measured at 650 nm with a spectrophotometer.

Results

Optimization of Thiolation Reaction. The extent of thiolation was analyzed after separation of the excess reagent from the product by gel filtration. The 2-iminothiolane-modified chitosan (chitosan-SH) was eluted in fractions 4−9 (Figure 1), and DTT and decomposed 2-iminothiolane were eluted after fraction no. 10 (data not shown). Thiolation, in duplicates, for 4, 6, and 10 h resulted in modification of 17.1, 18.2, and 20.2% of the amino groups (equivalent to 807, 860, and 953 μequiv SH/g chitosan), respectively. The optimal temperature for this reaction was 50−55 °C (Figure 2). To evaluate solubilization during the reaction from 0 to 4 h, $A_{650\ nm}$ was measured. During the course of thiolation, turbidity rapidly decreased within 1 h to the minimum value and remained so until 4 h.

Final Optimized Reaction of Chitosan with 2-Iminothiolane. Two hundred microliters of the chitosan suspension in buffer B (5.67 μequiv of NH_2 group) was mixed with 50 mg of 2-iminothiolane (363 μmol) and 800 μL of 2% DTT (104 μmol), and the reaction was kept for 7 h at 55 °C with

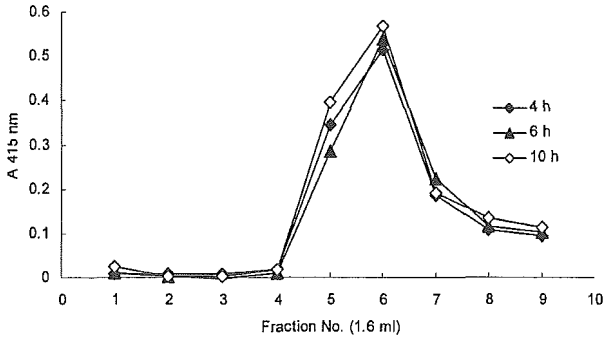

Figure 1. Separation of the reaction mixture of chitosan and 2-iminothiolane (4, 6, and 10 h) by Sepharose CL-6B (1 × 24 cm). Chitosan-SH was eluted in fractions 4–9.

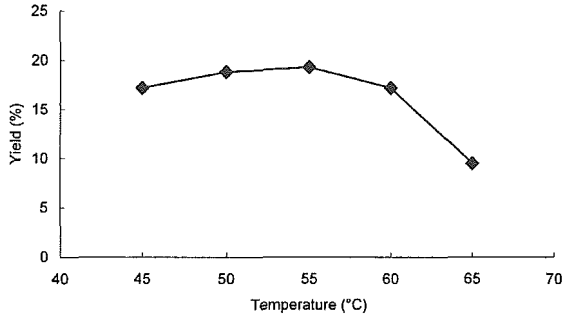

Figure 2. Thiolation yields of chitosan as a function of reaction temperature.

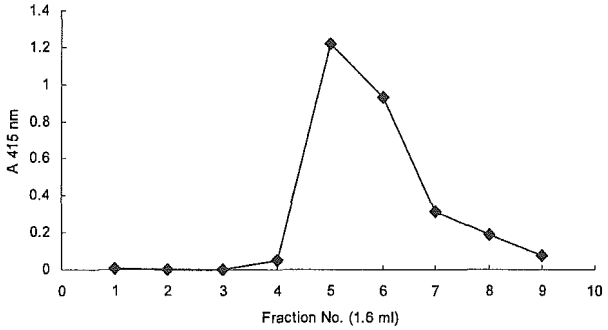

Figure 3. Separation of the mixture of chitosan and 2-iminothiolane by Sepharose CL-6B (1 × 24 cm). Chitosan-SH was eluted in fractions 4–9.

constant agitation. Purification of the product by gel filtration yielded the chitosan-SH, eluted in fractions 4–9 (Figure 3). Analysis of thiol, in duplicates, in the product indicated 19.3% modification of the amino group, which is equivalent to 913 μequiv SH/g chitosan, or 457 nequiv SH/nmol chitosan.

Turbidity of Chitosan from pH 3 to pH 6 and Chitosan-SH from pH 7 to pH 10. When chitosan samples were exposed to pH 3.0 and 4.0, it remained totally clear and showed virtually no absorbance (0.008 and 0.011, respectively) at 650 nm, while those exposed to pH 5.0 and 6.0 became visibly turbid, manifesting absorbance at 650 nm (0.149 and 1.081, respectively). One milliliter of chitosan-SH (86.7 nequiv/mL) was adjusted to pH 7.0, 8.0, 9.0, and 10.0 with 0.1 M Na_2CO_3. After standing at 20–22 °C for 1, 6, 24, and 168 h, the turbidity was assessed by $A_{650\ nm}$. The

Scheme 2. Sulfo-EMCS Reacting with BSA To Produce MalN-BSA

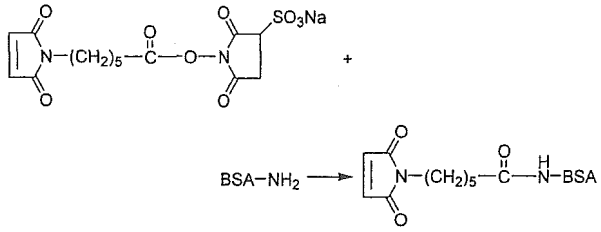

chitosan-SH was visibly clear at all times over the range of pH 7.0–10.0 and showed almost no absorbance at $A_{650\ nm}$ after 168 h.

Modification of BSA with Sulfo-EMCS. Sulfo-EMCS and BSA were dissolved in buffer B. To each of four solutions of BSA (1 mg in 1 mL) was added 0.4 mg (67.6 mol sulfo-EMCS/mol BSA), 1.0 mg (169 mol sulfo-EMCS/mol BSA), 2.0 mg (338 mol sulfo-EMCS/mol BSA), and 4.0 mg (676 mol sulfo-EMCS/mol BSA) of sulfo-EMCS, and the mixture was kept in the dark for 2 h at 20–22 °C (Scheme 2). After the reaction, each mixture was applied to a Sephadex G-50 column (1 × 25 cm), equilibrated and eluted in buffer B, at 1.5 mL/min, the effluent being monitored by $A_{260\ nm}$, and 1.6-mL fractions were collected. The MalN-BSA was eluted in the fraction nos. 5 and 6.

Determination of the Efficiency of the Conjugation of Sulfo-EMCS with BSA. Partis et al.[60] reported that the rates of reaction of the succinimido maleimides with β-mercaptoethanol could be followed spectrophotometrically by measuring the decrease in maleimide absorbance at 300 nm (molar absorption = 620 M^{-1} cm^{-1}) resulting from thioether formation. Following this, $A_{300\ nm}$ of the maleimide group was utilized in quantification of maleimide incorporated into BSA. The $A_{300\ nm}$ value of samples (fraction nos. 5 and 6) was corrected for the $A_{300\ nm}$ value contributed by BSA itself. Figure 4 shows the absorption spectra of MalNEt (0–500 nmol/mL), from which a standard curve of $A_{300\ nm}$ was constructed and analyzed by linear regression with Prism; $\hat{Y}$ = 0.000 654 4X − 0.001 595, with 0.9994 as the coefficient of determination $(r^2)^2$ and 0.003 153 as the estimated standard deviation (s). The molar absorption coefficient of MalNEt thus determined was 649 M^{-1} cm^{-1}. Therefore, the calculated yields (mole MalN per mole BSA) of maleimide addition were 12.8 (67.6 mol sulfo-EMCS/mol BSA), 23.6 (169 mol sulfo-EMCS/mol BSA), 31.2 (338 mol sulfo-EMCS/mol BSA), and 36.8 (676 mol sulfo-EMCS/mol BSA), respectively (Figure 5).

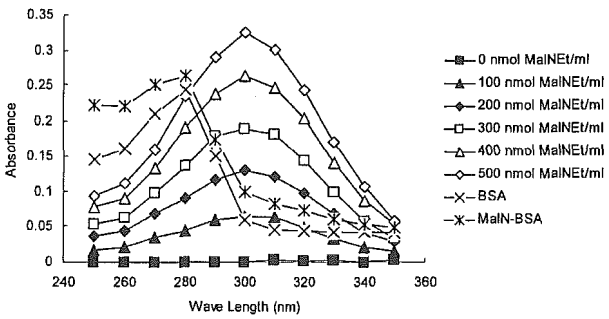

Figure 4. Absorption spectra of MalNEt, BSA, and MalN-BSA.

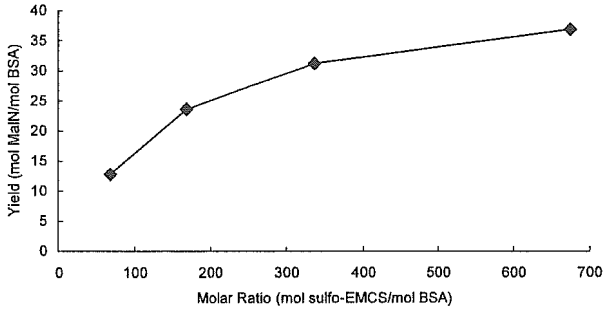

Figure 5. Modification of BSA with sulfo-EMCS of different concentrations.

Scheme 3. Chitosan-SH Reacting with MalN–BSA To Obtain Chitosan-S-BSA via Thioether Formation

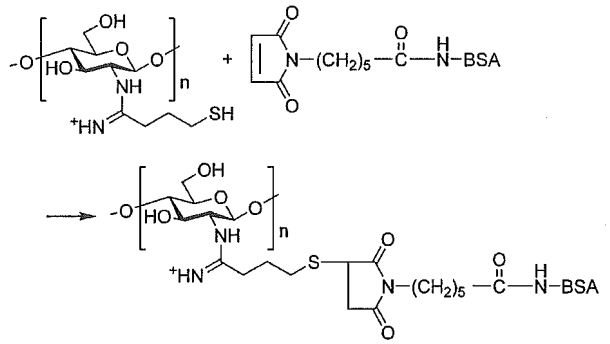

Conjugation of Chitosan-SH with MalN-BSA. One milliliter of chitosan-SH (244 nequiv of SH) was mixed with 1.5 mL of MalN-BSA (92.8 neqiuv of maleimide group), and the mixture was reacted in the dark for 3 h at 20–22 °C (Scheme 3). The reaction mixture was fractionated on the Sepharose CL-6B column as described above, except $A_{280\ nm}$ of the eluate was monitored. The chitosan-SH modified with MalN-BSA (chitosan-S-BSA) was eluted at fractions 4–7 (Figure 6).

The yield of the coupling reaction was estimated by measuring the unreacted SH group, and the amount of BSA conjugated to chitosan-SH was evaluated by $A_{280\ nm}$. By such analyses, in duplicates, 37.2% (90.8 nequiv) of the original SH group was consumed and 97.8% (90.8 neqiuv) of the maleimide (i.e., 6.76 nmol of BSA) group was reacted.

Quenching of the Residual SH Groups in Chitosan-S-BSA. The remaining SH group after the reaction of chitosan-SH with MalN-BSA was quenched by a large excess of bromoacetamide. Samples of chitosan-S-BSA (fraction nos. 4 and 5, 2.4 mL, and 94.7 nequiv of SH group) were reacted with bromoacetamide (1 mL of 3.3 mg/mL in buffer B, in a 250-fold excess of the SH group) for 2 h at 37 °C (Scheme 4), and the mixture was separated by the Sepharose CL-6B column. Quenched chitosan-S-BSA was eluted in fractions 3–5, and unreacted bromoacetamide was eluted in fractions 11–13. The thiol analysis of the eluted chitosan conjugate showed 20.0 nequiv, indicating that the efficiency of SH group quenching was 78.8%.

Discussion

In the current study, we chose to work with a chitosan of about 500 kDa, although it is easier to react with chitosans

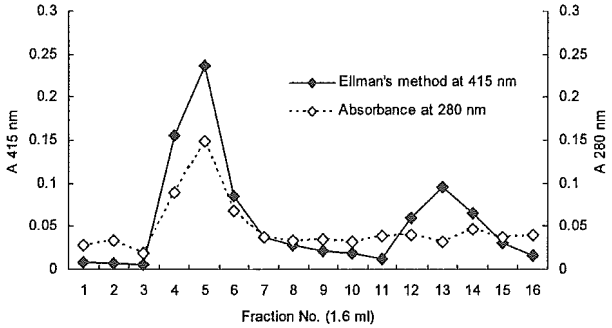

Figure 6. Purification of chitosan-S-BSA by the Sepharose CL-6B column.

Scheme 4. Quenching of Residual SH in Chitosan-SH with Excess Bromoacetamide

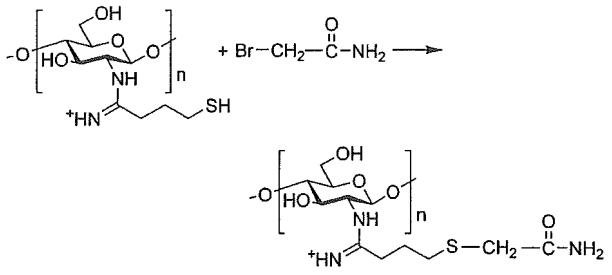

of lower molecular weights (Y. C. Lee, unpublished results). This is because our goal is to use chitosan in tissue engineering, and chitosans of higher molecule weight usually provide greater material strength.

Among many modifications of chitosan, the most recent report was by Bernkop-Schnürch et al.[49] In this method, 0.14% chitosan (83–85% deacetylated, 150 kDa) at pH 7 was reacted with 2-iminothiolane (0.58-fold over NH_2 group) for 24 h at room temperature under continuous stirring to attain 409 μequiv SH/g or 8.2% convertion of amino to thiol. For purification, the resulting conjugates were dialyzed. The gel prepared from such a chitosan-SH showed strong improvement in mucoadhesivity. We have now attained about 20% yield of thiolation (913 μequiv SH/g) by using more vigorous conditions of a higher molar ratio of 2-iminothiolane (NH_2 group of chitosan: 2-iminothiolane = 1:64) and a higher temperature, 55 °C, but for a shorter time. The speed of separation is quite important in avoiding oxidation of the SH group on chitosan-SH, and we purified the product with Sepharose CL-6B, which is faster and more efficient than dialysis, which Bernkop-Schnürch et al.[49] used for purification.

The thiolation yields for 4- and 10-h reactions are 17.1 and 20.2%. This means that chitosan is effectively modified with 2-iminothiolane and bestowed SH group from 0 to 4 h, when the reaction is slowed considerably. The reason for this slow down may be explained by conformational restrictions. Chitosan can be fabricated into nanoparticles by rapid stirring at room temperature with tripolyphosphate.[14,17,18] We can hypothesize that, during the thiolating reaction of chitosan, it becomes particulate and only outer amino groups would be thiolated.

Like Bernkop-Schnürch et al.,[49] we chose to use pH 7.0 for the thiolation reaction, because the pK_a of the amino

groups of chitosan is 6.3−6.5.[61,62] Chitosan as such is soluble only in acidic solution, which is not suitable for protein conjugation. At the beginning of the reaction at pH 7.0, the chitosan was not totally soluble, but as the reaction progressed, the suspension became clear. The chitosan-SH samples prepared by this method remained clear at pH up to 10.0. The solubilization of chitosan is due to formation of thiolate at pH above 7. The increased solubility of the thiolated chitosan permits its modification with other proteins, enzymes, glycoproteins, and proteoglycans at neutral to basic pH conditions. In fact, we have succeeded in efficient conjugation of BSA to chitosan-SH, by means of thioether formation via maleimide groups. This is the first report of covalent conjugation of a protein to chitosan. Our new method should find many applications in developing new chitosan-based biomedical materials containing other components such as growth factors, cell adhesion molecules, and the extracellular matrix.

References and Notes

(1) Illum, L. *Pharm. Res.* **1998**, *15*, 1326−1331.
(2) Rabea, E. I.; Badawy, M. E.; Stevens, C. V.; Smagghe, G.; Steurbaut, W. *Biomacromolecules* **2003**, *4*, 1457−1465.
(3) Jennings, C. D.; Boleyn, K.; Bridges, S. R.; Wood, P. J.; Anderson, J. W. *Proc. Soc. Exp. Biol. Med.* **1988**, *189*, 13−20.
(4) Sugano, M.; Fujikawa, T.; Hiratsuji, Y.; Nakashima, K.; Fukuda, N.; Hasegawa, Y. *Am. J. Clin. Nutr.* **1980**, *33*, 787−793.
(5) Nishimura, K.; Nishimura, S.; Nishi, N.; Saiki, I.; Tokura, S.; Azuma, I. *Vaccine* **1984**, *2*, 93−99.
(6) Sosa, M. A.; Fazely, F.; Koch, J. A.; Vercellotti, S. V.; Ruprecht, R. M. *Biochem. Biophys. Res. Commun.* **1991**, *174*, 489−496.
(7) Muzzarelli, R.; Tarsi, R.; Filippini, O.; Giovanetti, E.; Biagini, G.; Varaldo, P. E. *Antimicrob. Agents Chemother.* **1990**, *34*, 2019−2023.
(8) Qin, C.; Du, Y.; Xiao, L.; Li, Z.; Gao, X. *Int. J. Biol. Macromol.* **2002**, *31*, 111−117.
(9) Kato, Y.; Onishi, H.; Machida, Y. *Biomaterials* **2004**, *25*, 907−915.
(10) Vongchan, P.; Sajomsang, W.; Subyen, D.; Kongtawelert, P. *Carbohydr. Res.* **2002**, *337*, 1239−1242.
(11) Suzuki, M.; Itoh, S.; Yamaguchi, I.; Takakuda, K.; Kobayashi, H.; Shinomiya, K.; Tanaka, J. *J. Neurosci. Res.* **2003**, *72*, 646−659.
(12) Ma, L.; Gao, C.; Mao, Z.; Zhou, J.; Shen, J.; Hu, X.; Han, C. *Biomaterials* **2003**, *24*, 4833−4841.
(13) Tommeraas, K.; Strand, S. P.; Tian, W.; Kenne, L.; Varum, K. M. *Carbohydr. Res.* **2001**, *336*, 291−296.
(14) Huang, M.; Ma, Z.; Khor, E.; Lim, L. Y. *Pharm. Res.* **2002**, *19*, 1488−1494.
(15) Onishi, H.; Machida, Y. *Biomaterials* **1999**, *20*, 175−182.
(16) Kato, Y.; Onishi, H.; Machida, Y. *Biomaterials* **2000**, *21*, 1579−1585.
(17) Xu, Y.; Du, Y.; Huang, R.; Gao, L. *Biomaterials* **2003**, *24*, 5015−5022.
(18) Xu, Y.; Du, Y. *Int. J. Pharm.* **2003**, *250*, 215−226.
(19) Ishihara, M.; Obara, K.; Ishizuka, T.; Fujita, M.; Sato, M.; Masuoka, K.; Saito, Y.; Yura, H.; Matsui, T.; Hattori, H.; Kikuchi, M.; Kurita, A. *J. Biomed. Mater. Res.* **2003**, *64A*, 551−559.
(20) Park, Y. J.; Lee, Y. M.; Park, S. N.; Sheen, S. Y.; Chung, C. P.; Lee, S. J. *Biomaterials* **2000**, *21*, 153−159.
(21) Elcin, Y. M.; Dixit, V.; Lewin, K.; Gitnick, G. *Artif. Organs* **1999**, *23*, 146−152.
(22) Brown, C. D.; Kreilgaard, L.; Nakakura, M.; Caram-Lelham, N.; Pettit, D. K.; Gombotz, W. R.; Hoffman, A. S. *J. Controlled Release* **2001**, *72*, 35−46.
(23) MacLaughlin, F. C.; Mumper, R. J.; Wang, J.; Tagliaferri, J. M.; Gill, I.; Hinchcliffe, M.; Rolland, A. P. *J. Controlled Release* **1998**, *56*, 259−272.
(24) Richardson, S. C.; Kolbe, H. V.; Duncan, R. *Int. J. Pharm.* **1999**, *178*, 231−243.
(25) Roy, K.; Mao, H. Q.; Huang, S. K.; Leong, K. W. *Nat. Med.* **1999**, *5*, 387−391.
(26) Erbacher, P.; Zou, S.; Bettinger, T.; Steffan, A. M.; Remy, J. S. *Pharm. Res.* **1998**, *15*, 1332−1339.
(27) Liu, W. G.; Zhang, X.; Sun, S. J.; Sun, G. J.; Yao, K. D.; Liang, D. C.; Guo, G.; Zhang, J. Y. *Bioconjugate Chem.* **2003**, *14*, 782−789.
(28) Nishioka, Y.; Kyotani, S.; Okamura, M.; Miyazaki, M.; Okazaki, K.; Ohnishi, S.; Yamamoto, Y.; Ito, K. *Chem. Pharm. Bull. (Tokyo)* **1990**, *38*, 2871−2873.
(29) Sanzgiri, Y. D.; Blanton, C. D., Jr.; Gallo, J. M. *Pharm. Res.* **1990**, *7*, 418−421.
(30) Nishioka, Y.; Kyotani, S.; Okamura, M.; Miyazaki, M.; Sakamoto, Y.; Morita, M.; Okazaki, K.; Ohnishi, S.; Yamamoto, Y.; Ito, K. *Chem. Pharm. Bull. (Tokyo)* **1992**, *40*, 267−268.
(31) Mitra, S.; Gaur, U.; Ghosh, P. C.; Maitra, A. N. *J. Controlled Release* **2001**, *74*, 317−323.
(32) Degim, Z.; Celebi, N.; Sayan, H.; Babul, A.; Erdogan, D.; Take, G. *Amino Acids* **2002**, *22*, 187−198.
(33) Aiedeh, K.; Gianasi, E.; Orienti, I.; Zecchi, V. *J. Microencapsulation* **1997**, *14*, 567−576.
(34) Elcin, Y. M.; Dixit, V.; Gitnick, G. *Artif. Organs* **1998**, *22*, 837−846.
(35) Tomihata, K.; Ikada, Y. *Biomaterials* **1997**, *18*, 567−575.
(36) Peh, K.; Khan, T.; Ch'ng, H. *J. Pharm. Pharm. Sci.* **2000**, *3*, 303−311.
(37) Lahiji, A.; Sohrabi, A.; Hungerford, D. S.; Frondoza, C. G. *J. Biomed. Mater. Res.* **2000**, *51*, 586−595.
(38) Cui, Y. L.; Qi, A. D.; Liu, W. G.; Wang, X. H.; Wang, H.; Ma, D. M.; Yao, K. D. *Biomaterials* **2003**, *24*, 3859−3868.
(39) Zhu, H.; Ji, J.; Lin, R.; Gao, C.; Feng, L.; Shen, J. *J. Biomed. Mater. Res.* **2002**, *62*, 532−539.
(40) Wang, X. H.; Li, D. P.; Wang, W. J.; Feng, Q. L.; Cui, F. Z.; Xu, Y. X.; Song, X. H.; van der Werf, M. *Biomaterials* **2003**, *24*, 3213−3220.
(41) Yamane, S.; Iwasaki, N.; Majima, T.; Funakoshi, T.; Masuko, T.; Harada, K.; Minami, A.; Monde, K.; Nishimura, S. *Biomaterials* **2005**, *26*, 611−619.
(42) Iwasaki, N.; Yamane, S. T.; Majima, T.; Kasahara, Y.; Minami, A.; Harada, K.; Nonaka, S.; Maekawa, N.; Tamura, H.; Tokura, S.; Shiono, M.; Monde, K.; Nishimura, S. *Biomacromolecules* **2004**, *5*, 828−833.
(43) Muzzarelli, R. A.; Biagini, G.; Bellardini, M.; Simonelli, L.; Castaldini, C.; Fratto, G. *Biomaterials* **1993**, *14*, 39−43.
(44) Madihally, S. V.; Matthew, H. W. *Biomaterials* **1999**, *20*, 1133−1142.
(45) Suh, J. K.; Matthew, H. W. *Biomaterials* **2000**, *21*, 2589−2598.
(46) Nettles, D. L.; Elder, S. H.; Gilbert, J. A. *Tissue Eng.* **2002**, *8*, 1009−1016.
(47) Sechriest, V. F.; Miao, Y. J.; Niyibizi, C.; Westerhausen-Larson, A.; Matthew, H. W.; Evans, C. H.; Fu, F. H.; Suh, J. K. *J. Biomed. Mater. Res.* **2000**, *49*, 534−541.
(48) Muzzarelli, R.; Biagini, G.; Pugnaloni, A.; Filippini, O.; Baldassarre, V.; Castaldini, C.; Rizzoli, C. *Biomaterials* **1989**, *10*, 598−603.
(49) Bernkop-Schnürch, A.; Hornof, M.; Zoidl, T. *Int. J. Pharm.* **2003**, *260*, 229−237.
(50) Biagini, G.; Pugnaloni, A.; Damadei, A.; Bertani, A.; Belligolli, A.; Bicchiega, V.; Muzzarelli, R. *Biomaterials* **1991**, *12*, 287−291.
(51) Eser Elcin, A.; Elcin, Y. M.; Pappas, G. D. *Neurol. Res.* **1998**, *20*, 648−654.
(52) Varum, K. M.; Myhr, M. M.; Hjerde, R. J.; Smidsrod, O. *Carbohydr. Res.* **1997**, *299*, 99−101.
(53) Pangburn, S. H.; Trescony, P. V.; Heller, J. *Biomaterials* **1982**, *3*, 105−108.
(54) Hirano, S.; Tsuchida, H.; Nagao, N. *Biomaterials* **1989**, *10*, 574−576.
(55) Schipper, N. G.; Olsson, S.; Hoogstraate, J. A.; deBoer, A. G.; Varum, K. M.; Artursson, P. *Pharm. Res.* **1997**, *14*, 923−929.
(56) Biagini, G.; Bertani, A.; Muzzarelli, R.; Damadei, A.; DiBenedetto, G.; Belligolli, A.; Riccotti, G.; Zucchini, C.; Rizzoli, C. *Biomaterials* **1991**, *12*, 281−286.
(57) Chen, X. G.; Wang, Z.; Liu, W. S.; Park, H. J. *Biomaterials* **2002**, *23*, 4609−4614.
(58) Ueno, H.; Yamada, H.; Tanaka, I.; Kaba, N.; Matsuura, M.; Okumura, M.; Kadosawa, T.; Fujinaga, T. *Biomaterials* **1999**, *20*, 1407−1414.
(59) Ellman, G. L. *Arch. Biochem. Biophys.* **1959**, *82*, 70−77.
(60) Partis, M. D.; Griffiths, D. G.; Roberts, G. C.; Beechey, R. B. *J. Protein Chem.* **1983**, *2*, 263−277.
(61) El-Kamel, A.; Sokar, M.; Naggar, V.; Al Gamal, S. *PharmSci.* **2002**, *4*, E44.
(62) Kumar, G.; Smith, P. J.; Payne, G. F. *Biotechnol. Bioeng.* **1999**, *63*, 154−165.

BM049352E

ARTICLE IN PRESS

Available online at www.sciencedirect.com

SCIENCE DIRECT®

Biomaterials

ELSEVIER

Biomaterials ▮ (▮▮▮▮) ▮▮▮–▮▮▮

www.elsevier.com/locate/biomaterials

Chitosan–RGDSGGC conjugate as a scaffold material for musculoskeletal tissue engineering☆

Tatsuya Masuko[a,b], Norimasa Iwasaki[a,b], Shintaro Yamane[a,b], Tadanao Funakoshi[a,b], Tokifumi Majima[a,b], Akio Minami[a,b], Noriko Ohsuga[c], Takashi Ohta[c], Shin-Ichiro Nishimura[c,*]

[a]*Department of Orthopaedic Surgery, Hokkaido University School of Medicine, Kita-15, Nishi-7, Kita-Ku, Sapporo 060-8638, Japan*
[b]*Frontier Research Center for the Post-Genomic Science and Technology, Hokkaido University, Kita-21, Nishi-11, Kita-Ku, Sapporo 001-0021, Japan*
[c]*Laboratory of Bio-Macromolecular Chemistry, Division of Biological Sciences, Graduate School of Science, Frontier Research Center for the Post-Genomic Science and Technology, Hokkaido University, Kita-21, Nishi-11, Kita-Ku, Sapporo 001-0021, Japan*

Received 26 October 2004; accepted 25 January 2005

Abstract

In the present study, we have developed a novel and versatile method for the preparation of chitosan-peptide complex based on the selective reaction of chitosan with 2-iminothiolane. The new type of SH-chitosan derivative showed an excellent solubility to aqueous solution even in the alkaline conditions. This characteristic greatly facilitated further modification study of chitosan with a variety of bioactive substances. A synthetic peptide, RGDSGGC containing RGDS moiety that is known as one of the most important cell adhesive peptides, was readily coupled by disulfide bonds formation with sulfhydryl groups of SH-chitosan in the presence of dimethyl sulfoxide. Next, the effect of the introduction of RGDSGGC moiety to chitosan on cell adhesion and proliferation activity of chondrocytes and fibroblasts were evaluated. As a result, it was suggested that this polysaccharide-peptide conjugate exhibited excellent capacities for both cell adhesion and cell proliferation of chondrocytes and fibroblasts. Considering the growing importance of the biocompatible scaffolds in the recent tailored tissue engineering technique, these results indicate that the present strategy of 2-iminothiolane-based conjugation of polysaccharides with biologically active peptides will become a key and potential technology to develop desirable scaffold materials for the tissue regenerations.

Keywords: Adhesion; Chondrocyte; Fibroblast; Peptide; Polysaccharide

1. Introduction

The ideal treatment for severely injured tissues is that the involved tissues are replaced with functional ones. However, the current advanced treatments such as reconstructive surgeries and allogeneic transplantations have the possibility of occurring functional loss of a self-donor organ or tissue and lethal side effects derived from immunosuppressants. Recently, to overcome these limitations in the current treatments, various tissue engineering techniques have been developed for tissue regeneration [1–4].

The fundamental concept of tissue engineering technique is that a culturing isolated cell on a scaffold is transplanted into the target tissue for its regeneration [5]. Therefore, in tissue engineering, the importance of selecting the appropriate biomaterials as scaffolds for the cell attachment and supporting cell proliferation has been emphasized [6–15]. The biological tissues basically

☆A part of this work was presented at the 49th Orthopaedic Research Society, February, 2003, New Orleans, LA, USA, and the 50th Orthopaedic Research Society, March, 2004, San Francisco, CA, USA.

*Corresponding author. Tel.: +81 11 706 9043; fax: +81 11 706 9042.
E-mail address: shin@glyco.sci.hokudai.ac.jp (S.-I. Nishimura).

0142-9612/$ - see front matter © 2005 Elsevier Ltd. All rights reserved.
doi:10.1016/j.biomaterials.2005.01.062

consist of the cells and the extracellular matrix (ECM). It has been well documented that the interactions between the cells and the ECM are essential for various basic biological systems [16–19]. The ECM serves at least three functions in controlling cell behavior such as adhesion signals, growth factor binding sites, and degradation sites. Especially, interaction between the cells and their ECM plays an important role in hypocellular and hypo-vascular tissue regeneration such as cartilage and ligament tissue regeneration [1,13]. Although a variety of biomaterials, including naturally occurring, synthetic, or composite of the both, have been introduced as potential scaffolds, we believe that the ideal cell-carrier substance should be one that closely mimics the natural environment in the ECM.

It was subsequently shown that various ECM molecules contain specific peptide motifs that allow them to directly bind to cell surface receptors [20–24]. One of the best characterized motifs is the tri(tetra)peptide Arg-Gly-Asp-(Ser) [RGD(S)], first found in fibronectin. The peptides containing this amino acid sequence promote the adhesion of cells and inhibit the adhesive properties of fibronectin. On the other hand, integrins were the first identified ECM receptor. It is well established that, on the ligand binding, integrins can directly induce the biochemical signals into the cells. The cytoplasmic domain of the integrins interacts with the cytoskeleton, suggesting that the ECM signalings through integrins are transduced via the cytoskeletal elements and induce cell shape changes leading to the growth and/or differentiation. It is well known that RGD(S) motif of fibronectin could bind with integrin and the signal transduction was regulated through this RGD(S) motif.

Although cell adhesion molecules are crucial for the relationship between cells and ECM, little attention has been paid to their application to scaffold materials. Therefore, our attention was directed toward the mimicking the ECM functions through the conjugation of cell adhesive molecules to scaffold materials. For introducing functional molecules such as peptides, proteins, and carbohydrates, to stable scaffolds in order to acquire additional preferable interactions, functions, and specific cellular responses, Davis et al. reported three major methods of immobilization of biomolecules and cells [25]: physical adsorption, physical entrapment, and covalent attachment. The first and second approaches are physically based, while the third one is based on covalent or chemical attachment to the support molecules. Concerning sustainable tissue engineering, the immobilization must be preferable to last the time when damaged tissue is replaced with regenerating tissue. This long-standing immobilization of biomolecules to scaffolds will be achieved with covalent bonds. Although a number of methods have been developed for the conjugation of biomolecules to soluble or solid materials by covalent bonds, few methods are currently applied to develop a practically available scaffold material [25,26].

We focused on the effect of the introduction of cell adhesive peptides to chitosan on the cell adhesion and proliferation activity of this abundant aminopolysaccharide material. Chitosan had long been expected as one of the most potential polysaccharides for the biocompatible and wound healing materials [10,11,27–29]. The hypothesis of this study was that introducing the RGDS-containing sequence to this aminopolysaccharide could provide the versatile biocompatible scaffold materials with the enhanced cell adhesion and cell proliferation activities through the interaction with integrins. To test this hypothesis, for reasons mentioned above, we established a novel and efficient method to conjugate the RGDS-containing peptide with chitosan and evaluated its adhesivity and cell proliferation activity of chondrocytes and fibroblasts.

2. Materials and methods

2.1. Synthesis of RGDSGGC

A model peptide, Arg-Gly-Asp-Ser-Gly-Gly-Cys (RGDSGGC), was synthesized by solid-phase manner on Model 433A Peptide Synthesizer by Applied Biosystems (Foster City, CA, USA) using standard Fmoc/HOBt/DCC protocols. The Fmoc-L-amino acids and solvents used in the solid-phase peptide synthesis (SPPS) were purchased from Nova Biochem (Läufelfingen, Switzerland). The solid-phase synthesis was performed on HMP resin and trifluoroacetic acid (TFA), 1-hydroxybenzotriazole in *N*-methylpyrrolidone (HOBt in NMP) and dicyclohexylcarbodiimide in *N*-methylpyrrolidone (DCC in NMP) were used for the coupling reactions in dichloromethane (DCM) or dimethylformamide (DMF) as solvents. Deprotection and cleavage of the peptide from the resin were carried out by treating with 10 ml of reagent mixture containing 9.5 ml of TFA and 0.5 ml of water, for 3 h at room temperature. After releasing the products from the resin, the peptides were purified by HPLC. As shown in Fig. 1, the MALDI-TOF mass spectrum of fully deprotected and purified peptide was measured on an Ultraflex TOF/TOF mass spectrometer (Bruker Daltonics GmbsH, Bremen, Germany).

2.2. Introduction of the RGDSGGC to chitosan by means of 2-iminothiolane

Derivatization of chitosan with 2-iminothiolane was basically performed by employing the modified condition reported by Fu and Gowda [30], in which this

reaction was used for derivatization of some proteins [31–33] (Schemes 1 and 2). Four gram of chitosan powder (ca. 500 kDa, degree of deacetylation ca. 80%, Yaizu Suisankagaku Industry Co., Yaizu, Japan) was mixed with 1% acetic acid (200 ml) to make a 2% (w/v) stock chitosan solution (pH 2.68). Chitosan solution (3.5 g) was added to 50 mM potassium phosphate buffer solution (44 ml, pH 8.0) containing 2 mM EDTA and 150 mM NaCl. To a suspension containing chitosan was added with 2-iminothiolane (112 mg) and the mixture was incubated for 3 h at room temperature in a nitrogen atmosphere. The unreacted 2-iminothilane was removed by dialysis against distilled water with Seamless Cellulose Tubing (MWCO 12,000–14,000, Viskase Sales Inc., Chicago, IL, USA) for 7 days. Although the total volume of this reaction mixture increased to 68 ml after dialysis, it was found that the novel chitosan derivative showed much improved solubility to alkaline aqueous solution (pH 7–8, data not shown). Since this intermediate seemed to be easily converted into insoluble form by oxidative crosslinking even in an air atmosphere, we directly employed the homogeneous solution containing the key SH-chitosan intermediate for the subsequent disulfide bond formation with synthetic peptide as shown in Scheme 3. A synthetic peptide (45 mg of RGDSGGC in 6 ml of DMSO) was added to the solution of SH-chitosan prepared by the above-mentioned procedure (22.5 ml) according to the procedure reported by Tam et al. [34]. The mixture was incubated for 4 h at room temperature and subsequently dialyzed against distilled water for 7 days. Since the resulted solution was used as a stock solution for testing cell adhesion or proliferation assay, the half volume of the final solution was lyophilized to determine the precise concentration of the chitosan–RGDSGGC conjugate. As a result, the concentration of chitosan–RGDSGGC was estimated to be 0.12% (w/v). In the present study, the 96-well microtiter plates coated with this stock solution was termed as "0.12% hybrid".

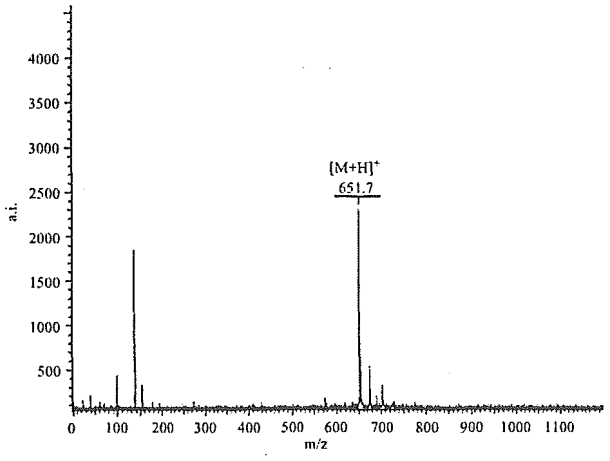

Fig. 1. MALDI-TOF mass spectrum of synthetic RGDSGGC.

2.3. Amino acid analysis

For the purpose of the determination of the degree of substitution by RGDSGGC moiety to SH-chitosan, amino acid analysis was carried out. The lyophilized sample was dissolved in 6 N HCl and placed in a thick-wall pyrex tube. The tube was then vacuum sealed and placed in the oven at 110 °C for 24 h. The hydrolysate was evaporated to dryness under reduced pressure and the residue was dissolved in 0.01 N HCl or citrate buffer (PIERCE, Rockford, IL, USA). The solution was loaded to the JLC/500V Amino Acid Analyzer (JEOL Ltd., Tokyo, Japan). Only the basic amino acids were analyzed on the basis of HPLC analysis.

2.4. Cell culture

Human articular chondrocyte of the knee was provided by BioWhittaker (Walkersville, MD, USA) and cultured in Chondrocyte Growth Medium Bullet-Kit®. Human fibroblast was provided by Cascade Biologics, Inc. (Portland, OR, USA) and cultured in medium containing Medium 106S®, LSGS®. Each medium was changed thrice a week.

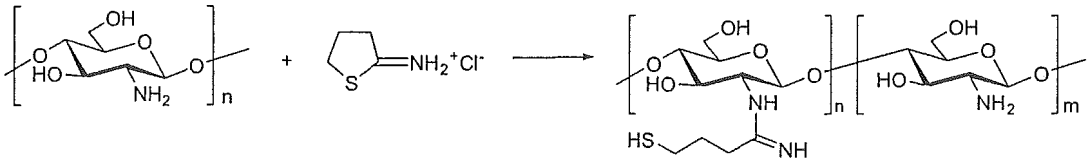

Scheme 1. Ring opening reaction of 2-iminothiolane with chitosan.

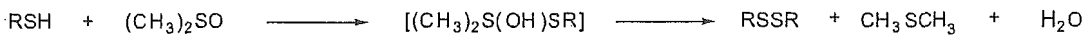

Scheme 2. DMSO initiated disulfide bond formation.